ON PAGE

Form Approved
OMB No. 0704-0188

Public reporting burden for this collection of information is estimated to average 1 hour per response, including the time for reviewing instructions, searching existing data sources, gathering and maintaining the data needed, and completing and reviewing the collection of information. Send comments regarding this burden estimate or any other aspect of this collection of information, including suggestions for reducing this burden, to Washington Headquarters Services, Directorate for information Operations and Reports, 1215 Jefferson Davis Highway, Suite 1204, Arlington, VA 22202-4302, and to the Office of Management and Budget, Paperwork Reduction Project (0704-0188), Washington, DC 20503.

1. AG

2. REPORT DATE
February 28, 1994

3. REPORT TYPE AND DATES COVERED
Reprint

4. TITLE AND SUBTITLE
Quiet-time Intensifications Along the Poleward Auroral Boundary Near Midnight

5. FUNDING NUMBERS
PE 61102F
PR 2311
TA G5
WU 02

6. AUTHOR(S)
O. de la Beaujardiere*, L.R. Lyons**, J.M. Ruohoeniemi#, E. Friis-Christensen##, C. Danielsen##, F.J.Rich, P.T. Newell#

7. PERFORMING ORGANIZATION NAME(S) AND ADDRESS(ES)
Phillips Lab/GPSP
29 Randolph Road
Hanscom AFB, MA 01731-3010

8. PERFORMING ORGANIZATION REPORT NUMBER
PL-TR-94-2041

9. SPONSORING/MONITORING AGENCY NAME(S) AND ADDRESS(ES)

*SRI International,Menlo Park,CA **Environmental Technology Center, Aerospace Corporation, Los Angeles, CA #Applied Physics Lab, Johns Hopkins Univ., Laurel, MD ##Hollandervaegnet, Dragoer, Denmark - Reprinted from Journal of Geophysical Research, Vol. 99, No. A1, pages 287-298, January 1, 1994

12a. DISTRIBUTION/AVAILABILITY STATEMENT
Approved for public release; Distribution unlimited

Radar and optical measurements from Sondrestrom are combined with satellite and Goose Bay data in a study of the poleward edge of the nightside auroral oval during a quiet period. The B_y and B_z components of the interplanetary magnetic field were close to zero, and the B_x component was −8 nT for more than 24 hours. On a large scale, the convection and precipitation patterns remained almost constant during this period; on a small scale, however, the conditions were quite dynamic. At 10- to 20-min intervals the arc that marked the poleward auroral boundary intensified, and a new arc appeared poleward of it. About once per hour, stronger intensifications were observed. One such event is examined in detail. The auroral arcs first appeared to dim, and then they brightened, with a factor of 10 increase in E region electron density. At the time of the brightening a new arc formed poleward of all the arcs. The arcs then drifted southward at velocities of ~270 m/s. A plasma drift disturbance, characterized by a doubling of the southward velocity and a reversal in the east-west component, propagated westward at 900 m/s through the fields of view of the Sondrestrom and Goose Bay radars. A simultaneous satellite overpass close to the radars revealed the presence of an energetic ion event similar to the "velocity dispersed ion structures" observed on the Aureol satellite and presumed to be the signature of fast ion beams within the plasma sheet boundary layer. The stronger arc intensification events observed by the Sondrestrom radar are associated with an increase in plasma flow across the boundary between open and closed magnetic field lines. We interpret this increased flow as the ionospheric signature of abrupt, localized increases in the reconnection rate in the midnight sector.

14. SUBJECT TERMS
Aurora, Ionosphere, Magnetosphere, DMSP, SondreStrom Fjord Plasma Sheet

15. NUMBER OF PAGES
12

16. PRICE CODE

17. SECURITY CLASSIFICATION OF REPORT	18. SECURITY CLASSIFICATION OF THIS PAGE	19. SECURITY CLASSIFICATION OF ABSTRACT	20. LIMITATION OF ABSTRACT
UNCLASSIFIED	UNCLASSIFIED	UNCLASSIFIED	SAR

JOURNAL OF GEOPHYSICAL RESEARCH, VOL. 99, NO. A1, PAGES 287-298, JANUARY 1, 1994

Quiet-time intensifications along the poleward auroral boundary near midnight

O. de la Beaujardière,[1] L. R. Lyons,[2] J. M. Ruohoniemi,[3] E. Friis-Christensen,[4] C. Danielsen,[4] F. J. Rich,[5] and P. T. Newell[3]

Radar and optical measurements from Sondrestrom are combined with satellite and Goose Bay data in a study of the poleward edge of the nightside auroral oval during a quiet period. The B_y and B_z components of the interplanetary magnetic field were close to zero, and the B_x component was ~8 nT for more than 24 hours. On a large scale, the convection and precipitation patterns remained almost constant during this period; on a small scale, however, the conditions were quite dynamic. At 10- to 20-min intervals the arc that marked the poleward auroral boundary intensified, and a new arc appeared poleward of it. About once per hour, stronger intensifications were observed. One such event is examined in detail. The auroral arcs first appeared to dim, and then they brightened, with a factor of 10 increase in E region electron density. At the time of the brightening a new arc formed poleward of all the arcs. The arcs then drifted southward at velocities of ~270 m/s. A plasma drift disturbance, characterized by a doubling of the southward velocity and a reversal in the east-west component, propagated westward at 900 m/s through the fields of view of the Sondrestrom and Goose Bay radars. A simultaneous satellite overpass close to the radars revealed the presence of an energetic ion event similar to the "velocity dispersed ion structures" observed on the Aureol satellite and presumed to be the signature of fast ion beams within the plasma sheet boundary layer. The stronger arc intensification events observed by the Sondrestrom radar are associated with an increase in plasma flow across the boundary between open and closed magnetic field lines. We interpret this increased flow as the ionospheric signature of abrupt, localized increases in the reconnection rate in the midnight sector.

1. Introduction

On the nightside, plasma and energy are generally transported from the region of open magnetic field lines in the polar cap to the region of closed magnetic field lines containing the plasma sheet. The rate of this transfer is controlled by the electric field along the boundary between open and closed field lines. The poleward boundary of the aurora is generally expected to lie at or equatorward of the open-closed field line boundary, and it is the feature closest to the field line boundary that can routinely be monitored from the ground.

In a previous paper [*de la Beaujardière et al.*, 1991] we initiated a study of auroral activity and plasma transport in the vicinity of this boundary by examining Sondrestrom radar data during two substorm periods. Here we analyze the auroral activity and plasma transport in the vicinity of the poleward boundary of the aurora during a prolonged quiet period, when the boundary remained almost continuously within the Sondrestrom radar field of view. During this period the interplanetary magnetic field (IMF) was unusually stable and almost exclusively sunward. This IMF orientation, nearly antiparallel to the solar wind velocity, corresponds to a very small interplanetary electric field, which should lead to very small electric fields over the region of open, polar cap field lines. *Luhmann et al.* [1984] and *Hoffman et al.* [1988] have argued that this IMF orientation corresponds to geomagnetic quiescence, because the coupling of solar wind energy into the magnetosphere is small.

We combine observations from the Sondrestrom incoherent scatter radar, the Goose Bay HF radar, the DMSP satellite, and ground-based magnetometers, as well as an all-sky camera and a scanning photometer at Sondrestrom. We show that repeated auroral intensifications took place at this boundary at 10- to 20-min intervals, and that larger intensifications took place every hour or so that were accompanied by enhanced equatorward flow.

We address the following questions: To what extent is the ionosphere steady during quiescent periods of stable IMF? How does the poleward edge of the aurora change with time? What is the intensity of the plasma flow and how does it vary? What are the temporal and spatial characteristics of very dynamic events that propagated through the combined fields of view (FOV) of the Sondrestrom and Goose Bay radars? Are these events associated with small-duration episodes of increased reconnection rate in the magnetotail? In what way are these events distinct from substorms?

We compare our results to global studies of energy transfer rates between the solar wind, the magnetosphere, and the ionosphere [*Baker et al.*, 1985; *Baker*, 1992; *Bargatze et al.*, 1985; *Klimas et al.*, 1992]. Two timescales have been uncovered in these works: a dominant one, near 1 hour, and a secondary one near 20 min. The observations presented here might offer an illustration as to how this bimodal response is manifested in detailed local observations.

[1]SRI International, Menlo Park, California.
[2]Enviromental Technology Center, Aerospace Corporation, Los Angeles, California.
[3]Applied Physics Laboratory, Johns Hopkins University, Laurel, Maryland.
[4]Hollandervaenget, Dragoer, Denmark.
[5]Geophysics Directorate, Phillips Laboratory, Hanscom Air Force Base, Massachusetts.

Paper number 93JA01947.
0148-0227/94/93JA-01947$05.00

2. Experiment Description and Overall Conditions

The Instruments

The observations took place on January 12 to 13, 1989. The data are primarily from the Sondrestrom incoherent scatter radar located on the western coast of Greenland (66.99 N, 50.95 W) at an invariant latitude of 74.1° [*Kelly*, 1983]. A number of ionospheric parameters are measured by the radar as a function of height and latitude, including the electron density, the ion and electron temperatures, and the plasma velocity. The radar was operated in successive elevation scans in the direction perpendicular to the local L shell, as described by *de la Beaujardière et al.* [1991]. Either full or half scans to the south of the radar were performed, with resolutions of 5 and 3 min, respectively. The radar was operated in this continuous elevation scan mode for a 10-hour period centered near magnetic midnight.

The Goose Bay HF radar (53.4 N, 60.4 W) looks over northeastern Canada and Greenland [*Greenwald et al.*, 1985]. The experiment mode was similar to that described by *Ruohoniemi et al.* [1991]. The phased-array antenna was stepped through 16 beam positions spanning a 50° azimuth sector centered on 5°N. The scan repeat time was varied between 96 and 192 s. The frequency used was 11.3 MHz. The radar detects backscatter from decameter-scale plasma density irregularities in the high-latitude F region. The Doppler shifts in the signal can be used to infer the line-of-sight component of the convective drift [*Ruohoniemi et al.*, 1987].

The DMSP F8 and F9 satellites were in operation at this time. Their orbits are sun-synchronous and circular near 840 km altitude. Their ascending and descending nodes were at 0600/1800 and 1030/2230 LT, respectively. They were equipped with an ion drift meter to measure the cross-track vertical and horizontal components of the ionospheric bulk flow [F. Rich and M. Hairston, Large-scale convection patterns observed by DMSP, submitted to *Journal of Geophysical Research*, 1993), and with ion and electron particle detectors sensitive to the energy range 32 eV to 32 keV, which are always oriented toward local zenith [*Hardy et al.*, 1984].

Geophysical Conditions

The observations took place when the IMF was remarkably constant and almost exclusively oriented in the sunward direction for a period of approximately 30 hours. Both the Y and Z components were very small, as illustrated in Figure 1. The overall plasma convection, as measured by the radars and the DMSP F8 and F9 satellites remained weak and stable. The maximum in the F8 potential drop across the polar cap was 35 kV (at 2330 UT). More typically, it was ~20 kV. The K_p index was small (2, 1-, 1-) during the period of radar operation and had been < 2 for the preceding 11 hours.

A number of criteria have been selected to classify a period as "quiescent." (See *Kerns and Gussenhoven* [1990, and references therein].) For example, *Lundin et al.* [1992] have defined quiescence as times when $B_z \sim 0$; *Hoffman et al.* [1988] have used an arbitrary threshold in the maximum ΔH magnetogram deviation and examined the DE global images. Indices used to define quiescent periods are also the AE or the hemispheric power index [*Foster et al.*, 1986], but neither are available for this study. We examined the magnetograms from the Greenland chains and EISCAT cross. During the 24-hour period from 1800 UT on January 12 to 0800 UT on January 13 (see Figure 1), the maximum $|\Delta H|$ deviations recorded were 80 γ in the east coast Greenland chain (~0015 UT), 60 γ in the EISCAT cross (~2100 UT), and only 30 γ in the Greenland west coast chain, which includes Sondrestrom, (at ~2115 UT). Therefore, this period might not have passed the Hoffman et al. criteria, who have set ΔH thresholds at 20 and 35 γ. We would not expect it either, because their study corresponded to periods of B large and positive whereas here, $B_z \sim 0$. The stringent criteria of *Kerns and Gussenhoven* [1990] for defining the ground state of the magneto-

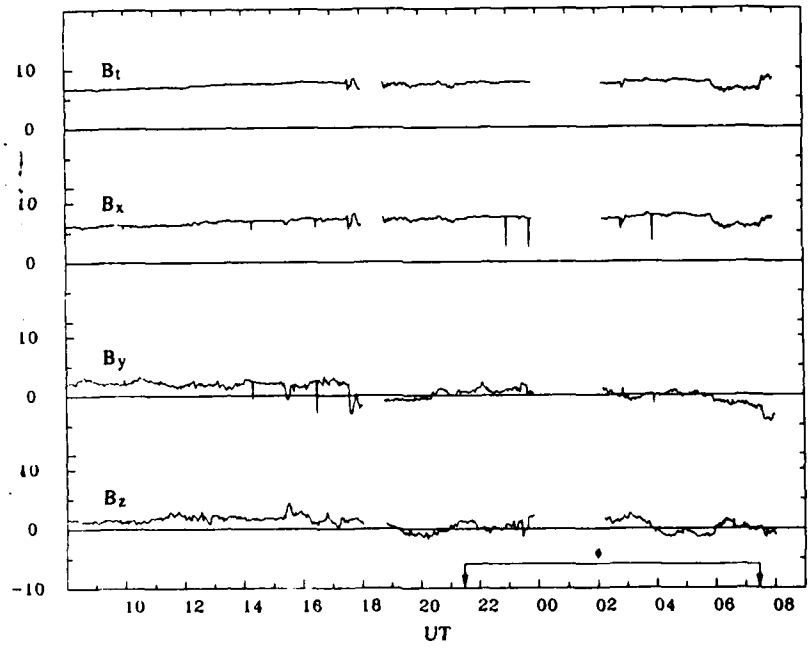

Fig. 1. IMF components in GSM coordinates, January 12-13, 1989. The Sondrestrom radar operation period, centered around magnetic midnight (diamond), is indicated at the bottom. The data are from the IMP 8 satellite, located at the GSM coordinates of -36, 4, 14 R_e.

sphere were not met either. Therefore, our data set corresponds to quiet conditions, but it does not correspond to a period of absolute quiescence.

Figure 2 shows the overall condition at Sondrestrom, which was on the nightside (0200 UT corresponds to magnetic midnight). The poleward edge of the auroral precipitation, as measured by the presence of ionization below 150 km altitude, remained almost entirely within the Sondrestrom radar field of view between 72° and 74° latitude. This is illustrated by the top panel in Figure 2 which displays the electron density at 150 km altitude as a function of UT. The Polar Anglo-American Conjugate Experiment (PACE) magnetic latitude [*Baker and Wing*, 1989] is used throughout the paper. This coordinate system is based on the International Geomagnetic Reference Field (IGRF) 1985 and is a smoothed variation of the corrected geomagnetic coordinate system.

The northward plasma velocity at 72.6° is shown in the bottom panel of Figure 2. The velocity was generally small, below 250 m/s, and mostly southward from 2315 to 0545 UT. However, there were repeated instances of enhanced southward flow, up to 500 m/s (e.g., near 0000, 0200, 0500 UT and a smaller enhancement near 0300 UT).

During the period of the Sondrestrom radar observations the Goose Bay radar detected echoes due to the presence of *F* region irregularities between 70° and 78° of PACE latitude. Also, the particle precipitation boundaries, as well as the precipitation intensities, measured by the two DMSP spacecraft did not change appreciably.

3. Precipitation Intensification Events

Sondrestrom Radar and Optical Data

Although large-scale patterns of convection and precipitation remained constant for the several hours shown in Figure 2, on a small spatial and temporal scale, conditions were quite variable. Figures 2 and 3 illustrate this point. Figure 3 shows data from four consecutive radar scans. These are half elevation scans performed from south to north with a 3-min cycle time. The upper part of Figure 3 displays the electron density in the magnetic meridian plane. At *F* region heights, electron density enhancements, often called blobs or patches, are seen to drift equatorward through the radar beam. Auroral arcs are identifiable from the enhancements in density below ~200 km. The poleward auroral oval boundary is a clear and well-defined feature.

By examining the radar data in conjunction with the all-sky camera (ASC) and the meridian scanning photometer, we can establish how the arcs move and when new arcs appear. During radar scan 1 the most poleward arc (labeled A) has a maximum electron density of 0.8×10^{11} electrons m^{-3}, and its poleward edge at 73.5° marks the poleward boundary of the auroral zone. A faint arc lies south of it. During scan 2, three minutes later, arc A has dimmed considerably; its electron density is decreased by 56% to 0.35×10^{11} electrons m^{-3}. This arc dramatically intensifies during scan 3, when the peak electron density is 10 times larger than during scan 2. A new arc, arc B, appears one degree poleward of the pre-existing arc A. During scan 4, arc B has brightened, and arc A has become fainter.

Between scans 1 and 2, the individual arcs do not appear to move much. However, between scans 2 and 4, they move southward at a velocity of about 270 m/s. The poleward boundary of the auroral oval moves poleward between scans 2 and 3, despite the southward motion of the arcs, as a result of the appearance of the new arc.

The north-south (N-S) component of the plasma drift for these four scans is also shown in Figure 3. During the first two scans this component is rather small, of the order of 100 to 200 m/s. It then increases, more than doubling in magnitude in the next two scans. The arc intensification and the formation of a new poleward arc are associated with this increase in the southward plasma velocity, which reached almost 500 m/s.

Data from the Sondrestrom scanning photometer and the ASC confirm the radar scenario: first the dimming of the poleward-most arc, and then its brightening and the appearance of a new arc poleward of it. Figure 4 displays four ASC photographs taken during the time of the Figure 3 data. The first photo, at 0152 UT, shows that the visual aurora almost totally disappeared during the period when the auroral precipitation was very weak (scan 2). The second photo (0154 UT) shows the brightening of arc A. The third (0156 UT) shows the appearance of the new arc, arc B, poleward of arc A. The fourth (0158 UT) shows the intensifica-

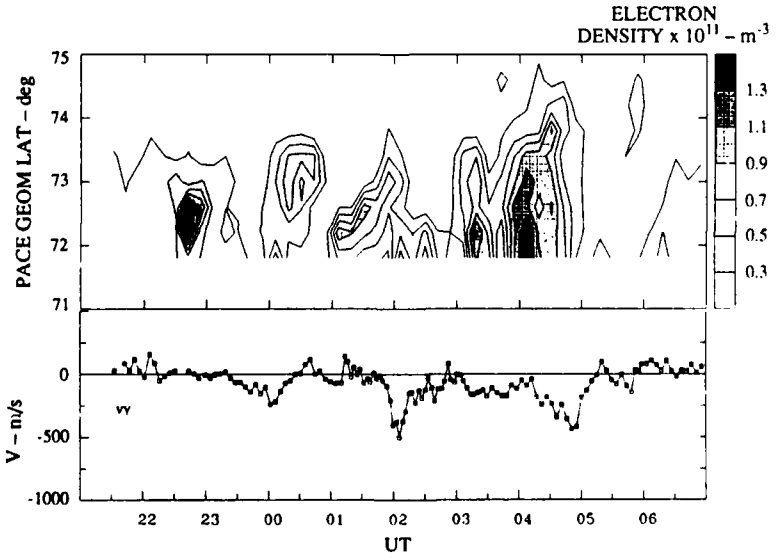

Fig. 2. Overview of the Sondrestrom observations during the period of January 12-13, 1989: Electron density at 150 km altitude, northward component of the ion drift at 72.6° Polar Anglo-American Conjugate Experiment (PACE) geomagnetic latitude.

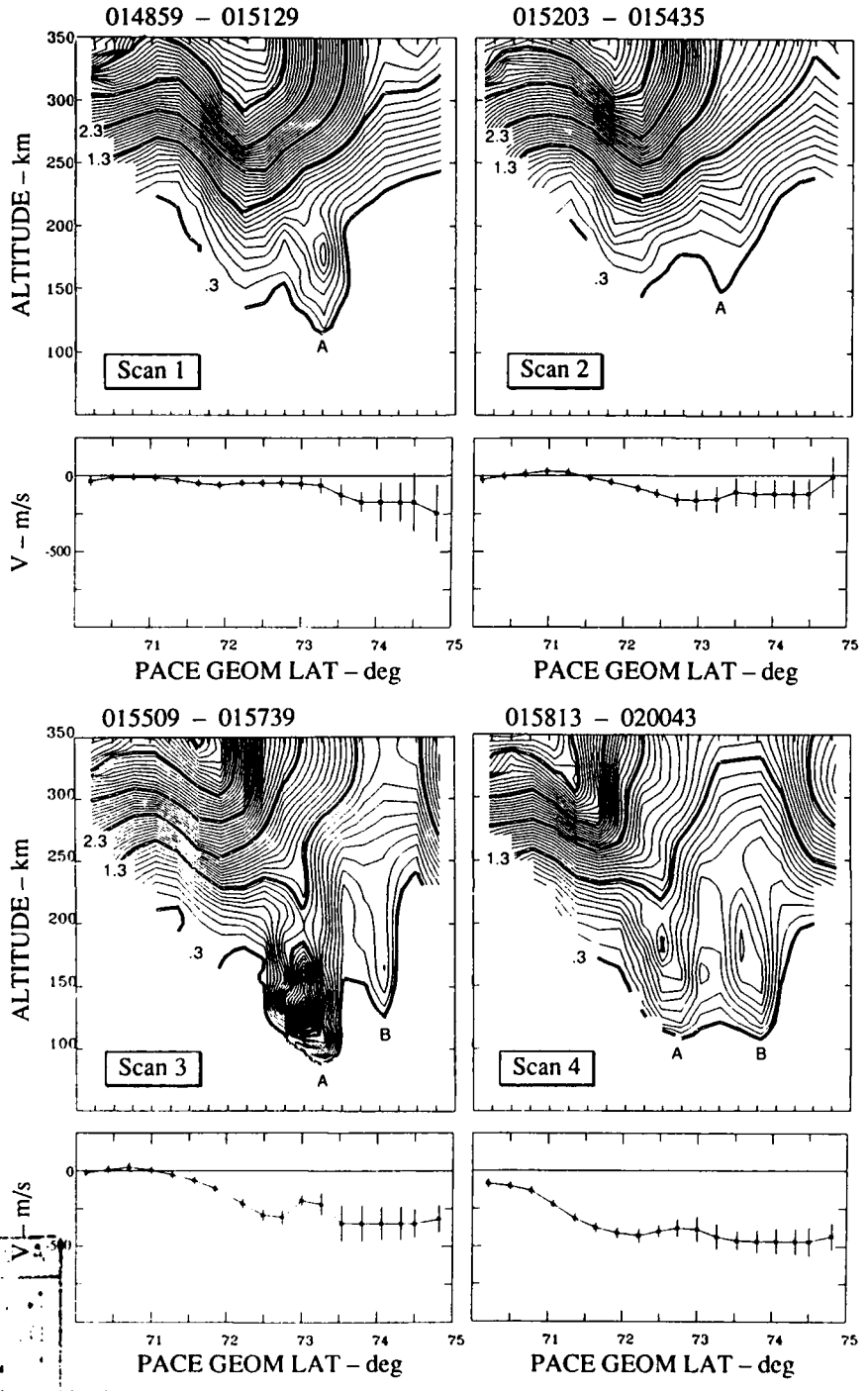

Fig. 3 Electron density contour plots and north-south ion drifts, measured by the Sondrestrom radar during each consecutive elevation scan, as a function of PACE geomagnetic latitude. The start and end times for each scan are indicated on the top. The vertical bars in the velocity panels are the statistical uncertainties.

tion of arc B. Although the timing of the radar scans was such that arc A appeared more intense than arc B, the scanning photometer and the ASC data revealed that the maximum intensities for arcs A and B were comparable.

The ASC photographs also reveal that the arcs were aligned approximately along L shells throughout this time period. Thus, the arcs seen by the radar in the meridian plane are not patchy auroral forms.

As mentioned, the Greenland West Coast magnetometer chain recorded very small magnetic deviations for this event. The latitudinal reversal from westward to eastward electrojet was probably between 72.6° and 73.7° magnetic latitude. The Sondrestrom magnetometer H (north) component slowly decreased by about 20 nT during the time when the plasma drift was large. This decrease was not characterized by the abrupt variation that typically accompanies a substorm expansion phase and the presence of a current wedge overhead of the station. Micropulsations were recorded at Sondrestrom during this event, but at a very low level (R. Arnoldy, private communication, 1992).

Similar sequences of events, that is, brightening of the poleward-most arc and appearance of a new arc poleward of it, occurred repeatedly during the night. This is illustrated by

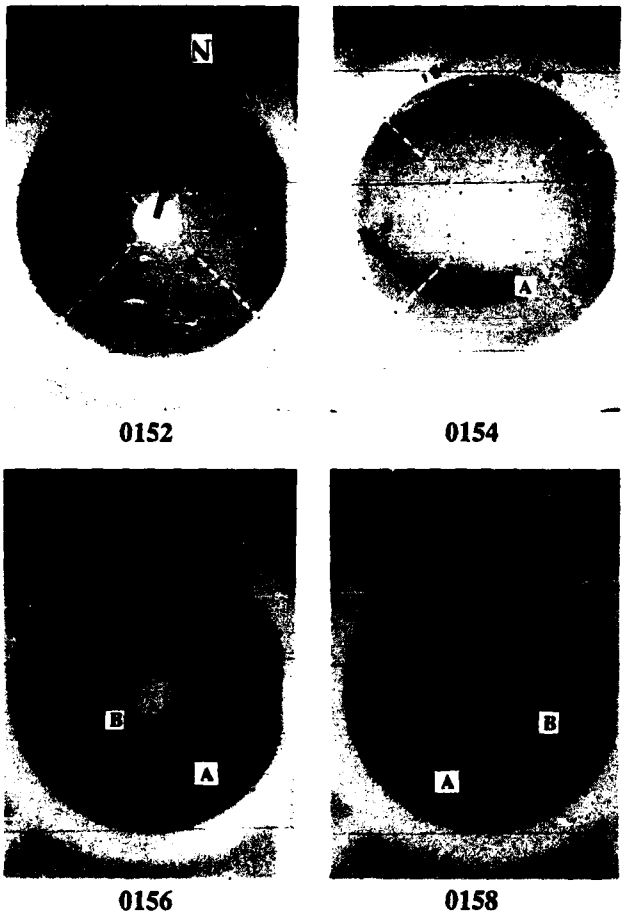

Fig. 4. Sondrestrom all-sky camera photographs taken during the time period of the four scans shown in Figure 3. North is at the top, east to the right.

Figure 5 which shows during a 3-hour period how the latitude of the poleward edge of the auroras changed as a function of time. The boundary is plotted at the latitude where the density falls below 0.3×10^{11} electrons m^{-3} at an altitude of 150 km. (Adopting a different height and density threshold would not affect our conclusions.) This boundary stayed within the radar field of view for the whole time period, except for two scans near 2340 UT, but it constantly moved back and forth.

A scan-by-scan examination of the density contour plots indicates that most boundary poleward motions were due to the formation of a new arc and that they were accompanied by an arc brightening. To illustrate this point, we have drawn a special symbol (a square within a circle) around the data points in Figure 5 each time a new arc appeared, and a different symbol (a square with a cross) each time an arc reached its maximum intensity. In most instances, both occurred either at the same time, or within one radar scan. The rapid poleward jumps of the boundary were usually followed by a more gradual equatorward motion of the boundary as the arcs drifted equatorward as, for example, between 0050 and 0120 UT.

Figure 6 shows the scanning photometer intensities at 557.7 and 630.0 nm for this time period. Each new arc that appears in the radar data is also evident in both wavelengths of the scanning photometer data, with a few exceptions—as when short-lived new arcs are only seen in the photometer data or when a new arc is too close to a pre-existing arc to be resolved in the photometer data. For example, the radar scans at 0112 and 0143 UT (dotted circles

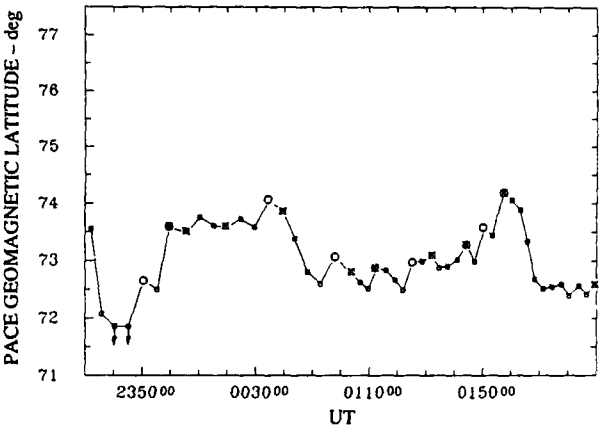

Fig. 5. PACE latitude of the aurora poleward boundary, as a function of time, for the 2330 to 0230 UT time interval, on January 12-13, 1989. The circle and cross symbols indicate times when a new arc appeared at the poleward edge of the auroral oval, and when an arc intensity reached a maximum, respectively. The two downward pointing arrows indicate that the boundary moved beyond the radar field of view.

in Figure 5) correspond to the formation of a new arc, as seen in the 6300 photometer data, but the radar data showed only a widening of the arc.

Overall, episodes of arc brightening and new-arc formation occurred 9 times during this 3-hour period, at irregular intervals that varied from ~10 to ~20 min. Similar sequences of events were observed for nearly 5.5 hours during the night, from 2330 to 0500 UT. Further toward the dusk and dawn sectors the electron precipitation was softer, and the poleward auroral oval boundary could not be located because it was difficult to distinguish between transported density patches and locally produced ionization from soft electron precipitation.

Most of the auroral brightening episodes marked in Figure 5 were not as intense as that of Figure 3. They typically corresponded to an increase in electron density from 0.4 to 1.4 10^{11} electrons m^{-3}. Once every hour or so, the intensity of the auroral brightening was much larger than usual, and was associated with a change in electric field, as exemplified in Figure 3. These stronger intensifications occurred around 0000, 0200, and 0310 UT; the last one, starting near 0400 UT, corresponded to continuous activity for 1 hour.

DMSP Data

In many respects, the larger intensification events have the same characteristic signature as substorms: magnetogram *H* component decrease, and auroral arc dimming followed by significant auroral intensification. The subsequent brightening of a more poleward arc (arc B in scan 4) following the initial arc brightening (arc A in scan 3) is also characteristic of substorms. Indeed, the existence of substorms at very high latitudes during periods of overall magnetic quiescence, has been reported before [*Akasofu*, 1973]. In other respects, however, these intensifications do not fit under the substorm label. Here the intensifications are observed on the most poleward arc, whereas during normal substorms it is the most equatorward arc that brightens at substorm onset [*Akasofu*, 1973; *Samson et al.*, 1992]. Also, the events do not show the abrupt decrease in the magnetogram *H* component typically associated with substorms.

We can further confirm that the perturbation observed at Sondrestrom did not propagate poleward from lower latitudes by examining a fortuitous DMSP overpass that crossed the radar

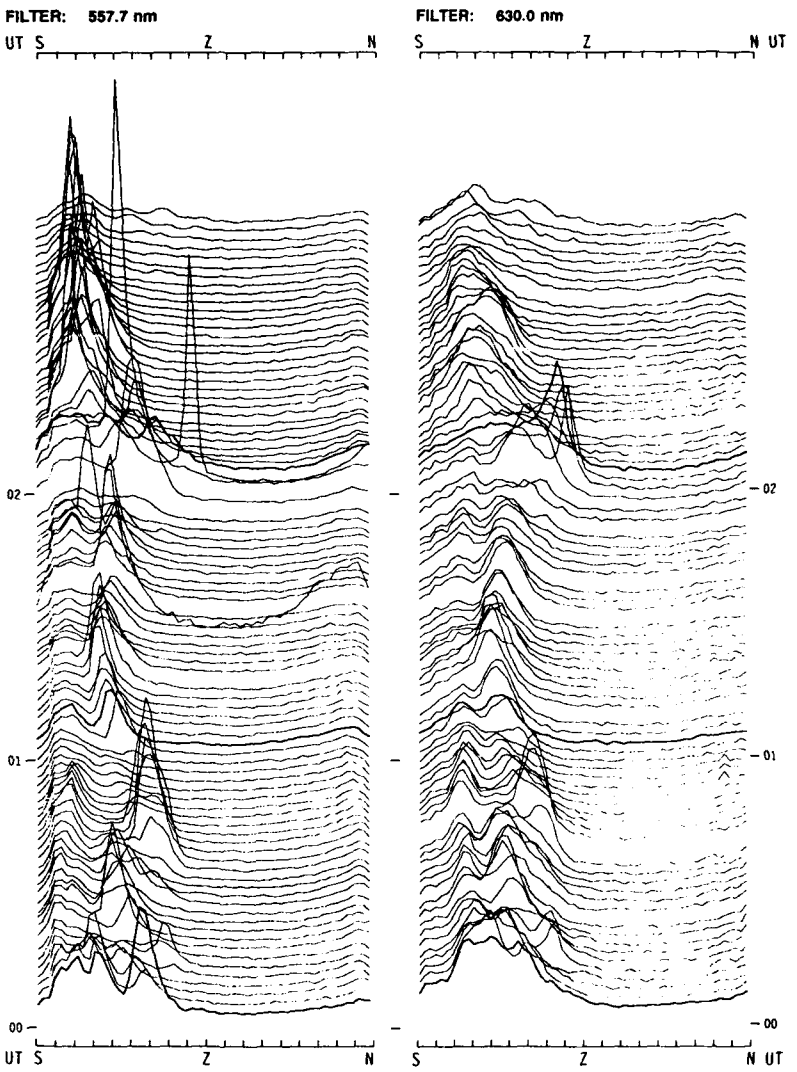

Fig. 6. Sondrestrom scanning photometer measurements at two wavelengths (557.7 and 630.0 nm) from 0000 to 0309 UT, on January 13, 1989. The abscissa is proportional to the photometric elevation angle. The heavy lines correspond to even universal time hours, and the traces are 2 min apart.

FOV from north to south a minute or two before the auroral intensification was observed. The DMSP ion and electron spectrograms versus time, PACE latitude and magnetic local time (MLT) are displayed in Plate 1. The precipitation regions indicated in Plate 1 correspond to the classification of *Winningham et al.*, [1975] and *Newell et al.* [1990]. The region where discrete auroral arcs are seen, labeled BPS (boundary plasma sheet), occupies the invariant latitudes between 73.0° and 67.4° (0152:32 and 0154:49 UT). The central plasma sheet (CPS) follows, much narrower (1.3°), and almost exclusively threaded by proton precipitation. Note that our use of Newell's terminology does not imply a one to one mapping between these particle populations and the actual regions in the magnetosphere from which they may originate [*Sandahl and Lindqvist*, 1990; *Galperin and Feldstein*, 1991], and, in particular, this "BPS" may not be related to the plasma sheet boundary layer described by *Eastman et al.* [1985].

The map in Figure 7 indicates the geometry of the satellite pass and of the Sondrestrom and Goose Bay radar data. It shows a two-dimensional snapshot of the line-of-sight plasma velocity measured from both radars. The satellite crossed the Sondrestrom radar FOV during scan 2, just prior to the arc intensification, and it was still within the auroral region at the beginning of scan 3, during which the intensification of arc A occurred. (The time of scan 2, between the letters B and E, is marked at the bottom of Plate 1.)

Throughout the pass, the intensity of the ion and electron precipitation is very weak, as are the average energies. The precipitation characteristics are similar to those observed during the passes that occurred before and after. There is no evidence of any significant auroral intensification during this pass. Specifically, there is no evidence during radar scan 2 for an intensification that would have occurred equatorward of arc A and propagated poleward so as to be observed during radar scan 3. This rules out the possibility that an auroral intensification first occurred at a lower latitude, closer to the equatorward boundary of the discrete auroral region, and subsequently moved to higher latitudes.

This DMSP pass provides another way to determine the orientation of the poleward edge of the auroral electron precipitation. This boundary is seen at the same PACE latitude, 73.6°, by both the satellite and radar, even though the satellite crosses it several degrees east of Sondrestrom, as shown in Figure 7. Therefore these data confirm that the auroral forms are east-west aligned.

The DMSP ion precipitation shows an unusual signature close to the poleward auroral oval boundary (0151:48 to 0152:31 UT

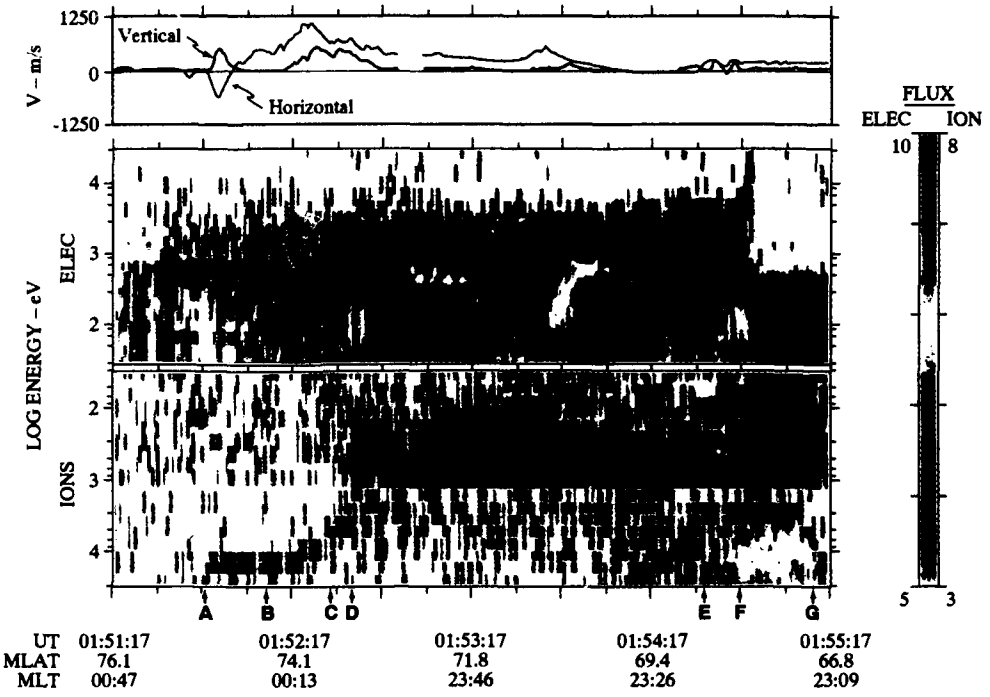

Plate 1. DMSP-F9 drift meter horizontal and vertical velocities, and spectrograms showing differential energy flux for electrons and ions (eV $(cm^2 s\ sr\ eV)^{-1}$) for January 13, 1989. The ion energy scale is inverted. The letters at the bottom indicate the particle regions and the time of the second scan of Figure 3, as follows: the boundary plasma sheet (BPS) lies between the C and F arrows; central plasma sheet (CPS) between F and G; scan 2 occurred between the times of B and E; and the energetic ion event took place between A and D (see text).

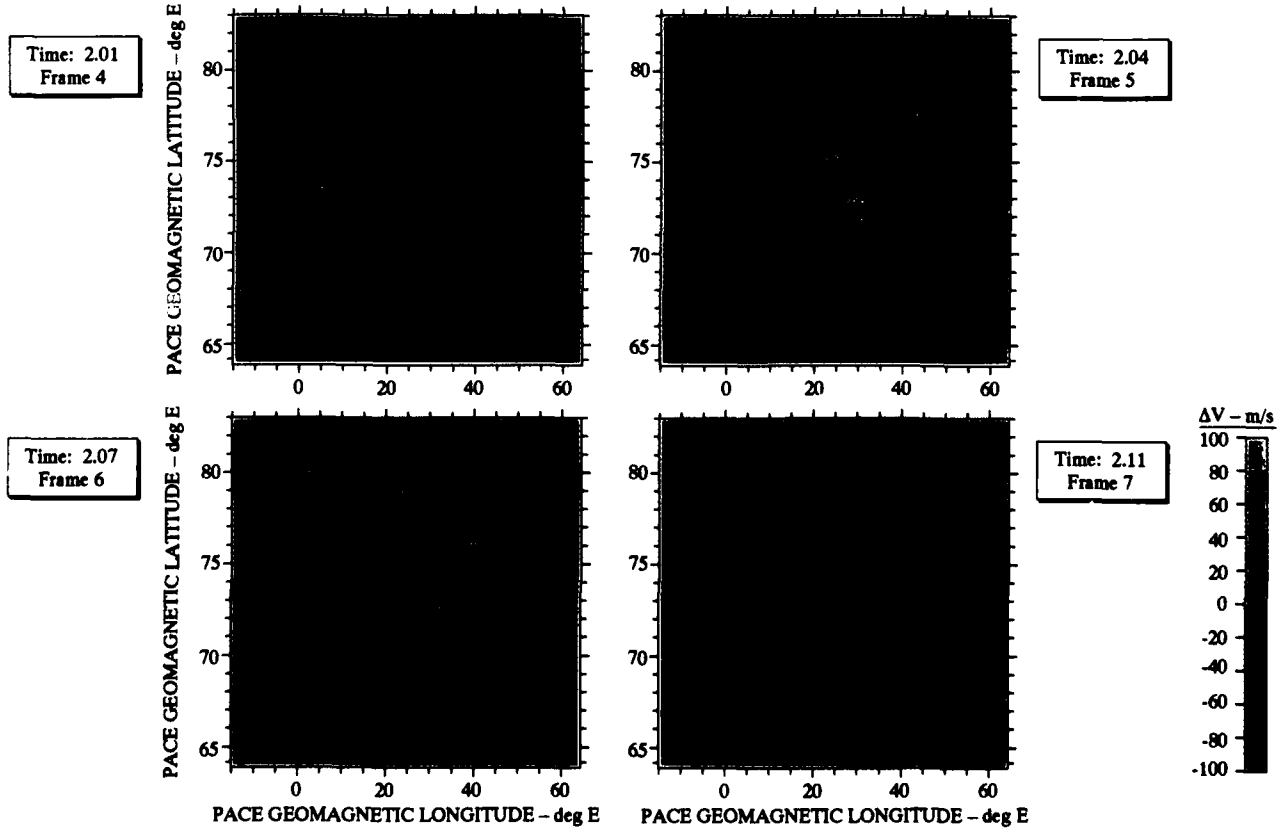

Plate 2. Propagation of the electric field perturbation through the Goose Bay radar field of view January 13, 1989. The gate-by-gate difference between the average and the measured line-of-sight velocity is shown for four consecutive scans versus PACE coordinates. The velocity difference goes from 100 m s^{-1} in the away direction, to 100 m s^{-1} in the toward direction, as the color symbols change from green to red.

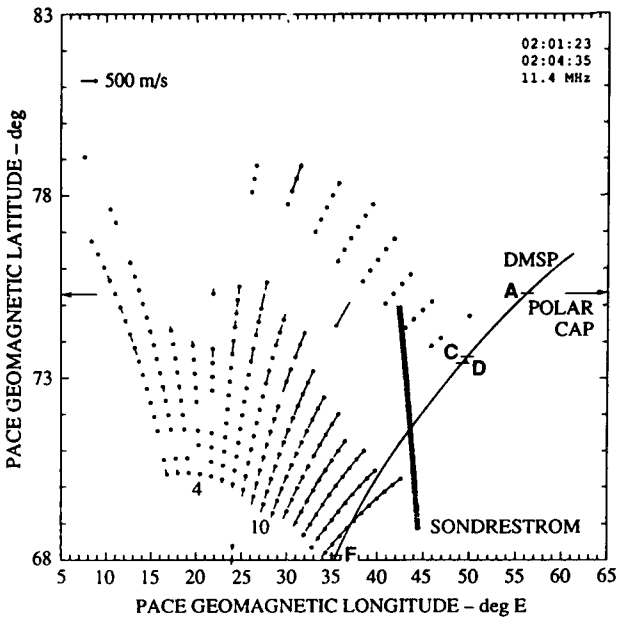

Fig. 7. Two-dimensional plot of the Goose Bay line-of-sight velocity, as a function of PACE coordinates (magnetic longitude and latitude) from 0201:23 to 0204:35 UT. The radar beams are numbered from east to west. The Sondrestrom radar field of view, and the DMSP-F9 trajectory for the pass shown in Plate 1, are also mapped. The points A through F along the satellite trajectory are those from Plate 1.

between the A and D arrows in Plate 1). At the most poleward latitudes of this ion event the ion distribution is monoenergetic. An examination of the individual spectra revealed that only one detector energy channel is affected, at 12.2 keV, with a number flux around 10^6 (cm^2 s sr eV)$^{-1}$. This monoenergetic trail is seen over approximately 1.2° in latitude, and then evolves into an ion dispersion curve, with the lowest energies seen at the lowest latitudes.

This type of ion signature is rare but not unique in the DMSP data. It might be similar to the velocity-dispersed ion structures (VDIS) studied by *Bosqued* [1987] and *Zelenyi et al.* [1990]. These structures are seen at the poleward edge of the auroras and have been interpreted as being due to the fast ion beams that drift earthward with velocities of 800 to 1800 km s^{-1} in the plasma sheet boundary layer (PSBL) [*Zelenyi et al.*, 1990; *Ashour-Abdalla et al.*, 1992] after being energized in the distant tail current sheet [*Lyons and Speiser*, 198?]. If this is the case, then the poleward edge of the ions (mark) is expected to be very close to the open-closed field line boundary. This boundary is indicated in Figure 7 as a tentative identification of the polar cap boundary.

The drift meter data for this pass are displayed in Plate 1, top panel. The horizontal drift, measured in the direction normal to the satellite trajectory, reverses from northwestward to southeastward as the satellite crosses the boundary. This confirms that the poleward edge of the ion event marks a significant boundary.

Propagation of the Electric Field Perturbation Through the Sondrestrom and Goose Bay Fields of View

To map out the electric field changes in time and space for this event, we now consider the Sondrestrom and Goose Bay radar velocity variations displayed in Figures 8-10, Plate 2, and Figure 11. Sondrestrom velocities at three latitudes are shown in Figure 8 as a function of time. Although the behavior at 70° dif-

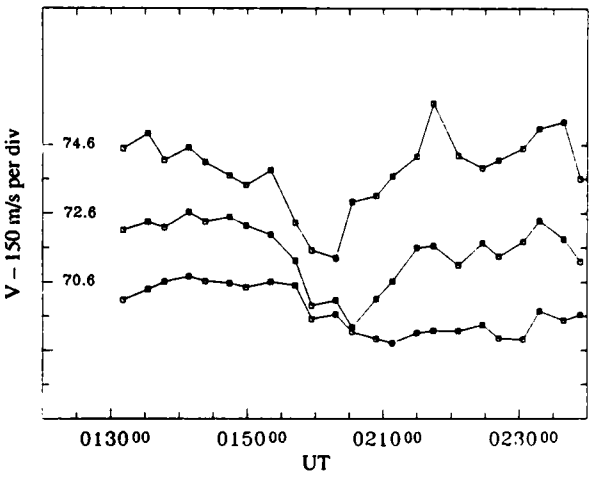

Fig. 8. Stack plot of the northward component of the Sondrestrom radar ion drift at three latitudes. Each plot origin is offset by two divisions. The perturbation is seen to propagate southward. For example, drift minima (black dots) occur later as the latitude decreases.

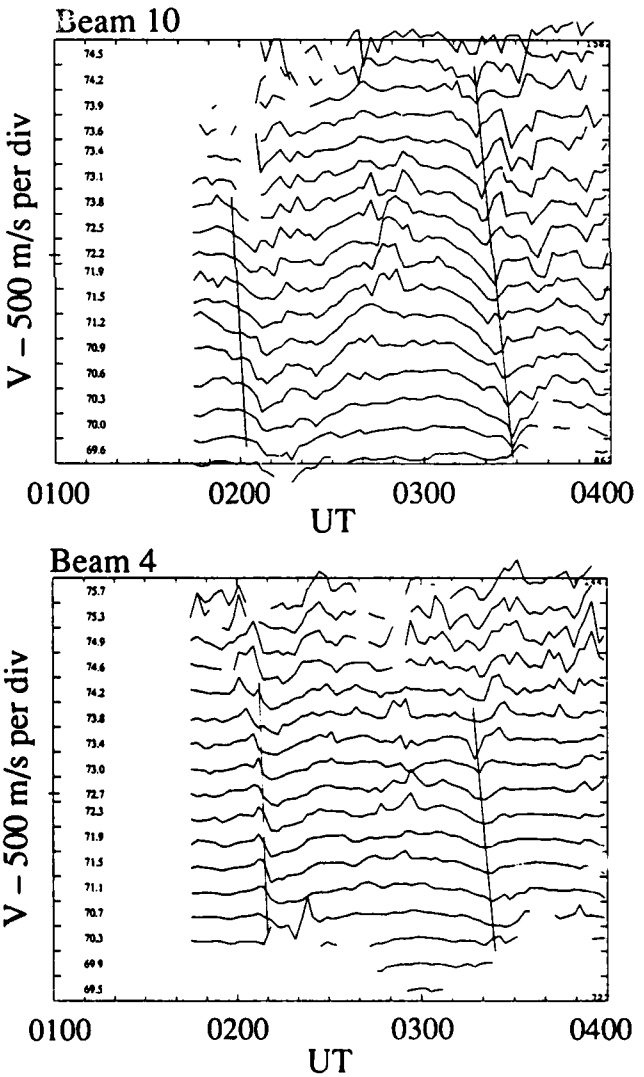

Fig. 9. Stack plots of the Goose Bay line-of-sight plasma drifts for each data gate along beams 10 and 4 (as numbered in Figure 7), with positive velocity for flow away from the radar. Along the ordinate axis, the tick mark separation indicates 500 m s^{-1} and the PACE geomagnetic latitude of each gate is given. Oblique lines through the velocity perturbations indicate how the perturbations propagate across the radar field of view.

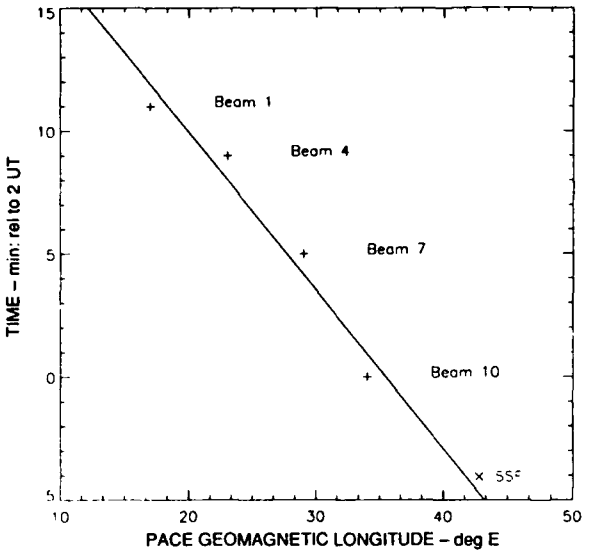

Fig. 10. Arrival time of the velocity perturbation as a function of PACE longitude, showing a westward propagation of the disturbance front from Sondrestrom (lower right) through four Goose Bay beams.

fers slightly from that at the other latitudes, there is a clear indication that the velocity perturbation is traveling southward through the field of view. From 74° to 70° the perturbation propagates at ~1000 m s^{-1}.

The Doppler velocity along two Goose Bay radar beams (those marked 10 and 4 in Figure 7) are shown in Figure 9. Stack plots of velocity versus time are shown for several gates from 70.5° to 80° PACE latitude. A southward velocity perturbation, similar to that at Sondrestrom (Figure 8), is evident ~0200 UT. The perturbation is first directed away, then toward the radar. It propagates westward from Sondrestrom through the field of view of Goose Bay. The propagation in the magnetic west direction is displayed in Figure 10, which shows the arrival time at a PACE latitude of 72.5° of the southward velocity increase at several longitudes across the FOV of the Sondrestrom and Goose Bay radars. These data are consistent with a uniform westward propagation speed of ~900 m/s. Note from Figure 9 a similar perturbation occurring near 0310 UT which is also seen in the Sondrestrom radar data near 0300 UT and which propagates through the FOV of both radars.

As was seen at Sondrestrom, the disturbances also move southward through the Goose Bay field-of-view. This is evidenced by the beam 4 data, since this beam is almost parallel to the magnetic meridian. (See, for example on Figure 9 between 71° and 74°). This southwestward motion is consistent with a propagation front that is inclined with respect to the north-south direction, and that propagates westward.

Plate 2 illustrates how this perturbation travels through the Goose Bay field-of-view. Four consecutive panels are shown (0201 to 0211 UT), similar to those of Figure 7, except that the color-coded values were calculated by subtracting, at each gate, the average from the measured Doppler velocity. First, a region of enhanced "away" flow moves in from the east, filling in nearly the entire southern half of the FOV by the time of the first panel. It is replaced by a region of significantly enhanced "toward" flow that can be seen to move from east to west.

Going back to Figure 9, one can see from beam 10, which makes a significant angle (~32°) with respect to geomagnetic north, that the east-west plasma velocity might have reversed as the disturbance passed across the Goose Bay FOV. For example,

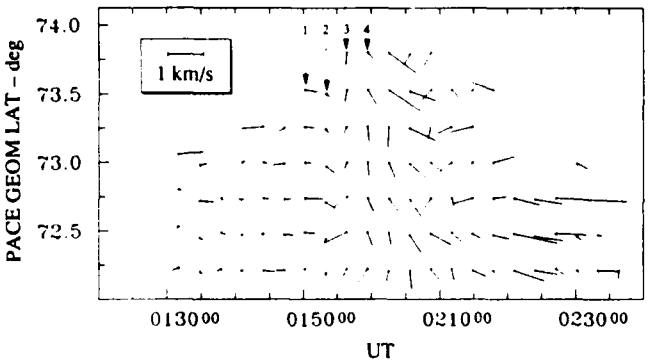

Fig. 11. Sondrestrom radar velocity vectors displayed as a function of time and PACE latitude, January 13, 1989. The numbers at the top refer to the four scans in Figure 3.

at 0215 UT, the line-of-sight velocity is large and <0 at low latitudes, and ≥0 at high latitudes. The Sondrestrom radar data support this assumption. The eastward plasma drift was calculated from the *E* region ion velocity using a technique described by *de la Beaujardière et al.* [1977], and the velocity vectors are plotted as a function of time and latitude in Figure 11. Complicated velocity rotations versus time as well as latitude are evident. The vector rotations during scans 3 and 4 correspond to a negative electric field divergence across the arc system, and thus to an enhanced upward Birkeland current. Therefore, the Goose Bay and Sondrestrom data are consistent and show that the electric field perturbation is associated with an auroral intensification.

It can be seen from Figures 7, 9, 10 and Plate 2 that the velocity perturbation covered a large portion of the Goose Bay FOV with a maximum extent within the FOV of both radars of approximately 30° in longitude by 9° in latitude. This area corresponds to a square roughly 1000 × 1000 km, and the actual perturbation could have covered a larger area. Furthermore, while high-latitude echoes received from Goose Bay were somewhat limited, the electric field perturbation clearly extended at times to latitudes poleward of the polar cap boundary inferred from the DMSP measurements.

Estimate of the Reconnection Rate

The reconnection electric field, as mapped into the ionosphere, can be evaluated by measuring the plasma velocity perpendicular to the estimated location of the polar cap boundary, in the boundary reference frame [*de la Beaujardière et al.*, 1991]. In the present case, we can readily estimate the flow rate across the poleward boundary of the aurora using the Sondrestrom data. This flow is in general small, consistent with the small interplanetary electric field during this time period. It increases significantly during the periods of enhanced southward velocity associated with the stronger auroral intensifications. On the basis of DMSP data, the actual boundary between open and closed field lines may have been ~2° in latitude poleward of the poleward auroral boundary as detected from *E* region density enhancements. The Sondrestrom latitude coverage was purposely limited during this time period to increase the experiment time resolution near the poleward boundary of the aurora. Thus the Sondrestrom radar was not scanning to the polar cap latitude inferred from DMSP. However, assuming that the location of the polar cap boundary did not have large variations with time or longitude, we can use the Goose Bay electric field.

Figures 7 and 9 show that the electric field at the boundary was generally quite weak, consistent with a small reconnection electric

field. Figure 9 indicates that the propagating electric field structure extended to latitudes above the polar cap boundary. During the time of the southward perturbation the reconnection electric field in the ionosphere increased substantially, reaching peak values of the order of 25 mV m^{-1}. This value for the reconnection electric field is only an estimate, but it is clear that the reconnection rate increased in association with the velocity disturbance structure. Since the southward plasma drift increased over a broad latitudinal range, an error in the polar cap boundary would not change this conclusion.

4. Summary and Conclusions

Observations at the poleward boundary of the aurora were made during a quiet period that lasted about 30 hours. During this period the IMF was oriented almost exclusively sunward. The DMSP ion and electron energy fluxes and the large-scale precipitation boundaries did not change appreciably during the observation interval. The potential drop across the polar cap remained very small. The small ionospheric electric fields are consistent with the fact that the electric field carried by the interplanetary medium is almost zero. However, this orientation does not correspond to a minimum in the area of open polar cap field lines, this area would have been smaller if B_z had been positive, and thus the poleward boundary of the auroras remained within the radars field-of-view during most of the observation interval.

Despite the overall conditions of quiet auroral activity and small electric fields, midnight sector observations revealed that the electric field and auroral precipitation were quite dynamic. Intensifications of the poleward most arc were observed every 10 to 20 min. These intensifications were associated with the poleward appearance of a new arc. Individual arcs drifted equatorward.

Approximately once per hour, stronger intensification events took place that had the following characteristics:

1. Fading of the most poleward arcs, followed by a rapid increase in precipitation (E region electron density increases by approximately an order of magnitude).

2. Formation of a new arc poleward of the pre-existing arcs, and equatorward motion of all arcs at a velocity of ~270 m s^{-1}.

3. Propagation of a southward plasma drift disturbance through the Sondrestrom and Goose Bay FOV. The plasma $\boldsymbol{E} \times \boldsymbol{B}$ southward drift more than doubled, and the disturbance propagated westward at speeds of ~1000 m s^{-1}.

4. This electric field disturbance is associated with an increase in the plasma flow across the poleward boundary of the auroral oval and appears to be associated with a local increase in the reconnection rate.

5. A DMSP pass revealed the simultaneous presence, poleward of the auroral electron boundary, of ion precipitation similar to the velocity-dispersed ion structure events that have been associated with the PSBL.

Previous studies have also shown that nightside auroral activity can take place at very high latitudes during geomagnetically quiescent periods. For example, substorms have been observed on contracted ovals [*Akasofu*, 1973] and auroral brightenings that repeat every 5 or 10 minutes have been observed at the boundary between diffuse and discrete auroras [*Sergeev et al.*, 1986]. Although the intensification events described here resemble substorms, they are probably a separate class of phenomena because the initial auroral breakup occurs along the poleward-most auroral arc rather than along a more equatorward arc.

These events are probably not rare, and they have some resemblance to other events described in the literature. *Williams et al.* [1993] observed rapid bursts in plasma convection using the European incoherent scatter (EISCAT) radar. However, those observations were mostly point measurements and gave little information on the spatial and temporal evolution of the convection bursts.

De la Beaujardière and Heelis [1984], using AE-C and Chatanika radar data, observed sudden increases in the equatorward convection. These events were located at the poleward edge of the auroras, and they might be similar to the events reported here. However, the cycle time of the Chatanika radar mode during these observations was too long to estimate how these electric field perturbations propagated, and how the associated auroral precipitation evolved.

Sergeev et al. [1990] described regions of enhanced southward ionospheric convection that propagate southward through the STARE radar beam. These events differ from those described here, in that the data correspond to active conditions, and no well-defined auroral structures could be identified in association with them (although the optical ASC data were contaminated by moonlight).

Similar events in terms of auroral precipitation were reported by *Pudovkin* [1991]. Auroral motions mapped out from a chain of ASC showed a behavior similar to what we have here: at the poleward edge of the auroral oval, arcs were usually drifting equatorward, and new arcs were being formed poleward of the pre-existing arcs. But again, these observations took place during active conditions.

Therefore events similar to ours have been observed before, but each observation was made with a different set of instruments, with different spatial and temporal resolutions, and under different geophysical conditions. We thus cannot conclude with certainty whether any of the previously reported events are the same as ours.

Interestingly, the intensification events reported in the present paper are similar in many respects to transient events observed at Svalbard near noon using optical instruments [e.g., *Sandholt*, 1990; *Fasel et al.*, 1992]: in the noon sector, at ~10-min intervals, arcs brighten, move poleward, and new arcs are formed equatorward of the pre-existing arc system. Coincident EISCAT observations show that these transient events are associated with increases in the poleward plasma convection [*Lockwood et al.*, 1989]. As expected, the dayside events have plasma convection and arc motion that are poleward around noon, whereas these motions are equatorward during our events near midnight. Also, the new arc that appears is equatorward of the pre-existing arcs around noon, and poleward around midnight. Therefore it is tempting to draw a parallel between the dayside and nightside events, and to associate the nightside events with transient increases in plasma transfer from open to closed field lines and the dayside events with transient increases in plasma transfer from closed to open field lines.

Williams et al. [1993] and *Sergeev et al.* [1990] also associated the transient events they observed with rapid increases of the nightside reconnection rate. The data we present give support to this interpretation. The ion-dispersion signature in the DMSP data indicates that the increase in reconnection might be associated with enhanced energization in the distant tail current sheet, as would be expected from an enhancement in the cross-tail electric field [*Lyons and Speiser*, 1982]. The ion fluxes could have been large enough to be detected by DMSP because the electric field in the distant tail increased significantly. In a way similar to reconnection on the dayside, our events are also associated with propagating electric field structures having enhanced vorticity that are

associated with an increase in the auroral precipitation. Our study, however, cannot reveal the exact nature of the magnetotail mechanisms that give rise to the ionospheric manifestations described here.

Our local observations can be considered in the context of large-scale statistical and theoretical investigations of the energy transfer between the solar wind and the magnetosphere. For example, the linear-filter predictions of *Bargatze et al.* [1985] have shown that the magnetosphere responds with two dominant timescales to changes in the solar wind input function: one near 20 min, and the other near 1 hour. This bimodal response is more pronounced for the lowest levels of input energy. These two time constants are remarkably similar to the frequency at which we have observed the small auroral intensifications, and the larger ones, respectively. Similar periodicities are apparent in simplified simulations of the magnetosphere such as electrical circuit [*Weimer*, 1992], Faraday loop [*Klimas et al.*, 1991; *Baker et al.*, 1991], or "dripping faucet" [*Baker et al.*, 1990] analogies. For example, the Faraday-loop analogue model revealed that when the energy input from the solar wind is constant, the energy is released episodically from the magnetotail regardless of the level of energy input [*Klimas et al.*, 1992]. In this analogue model the episodes of largest energy release occur with one-hour periodicity, while episodes of much smaller energy release occur at shorter intervals [*Baker et al.*, 1991]. Our observations apply to the low-energy end of these studies and appear consistent with their conclusions. In this respect the exact level of "quiescence" might not be important. Similar episodic releases of energy probably do take place during more active periods, as mentioned above, or during periods even more quiet than those encountered here.

Substorms are considered to be the manifestation of sudden, nondriven, release of the energy stored in the magnetotail [e.g., *Rostoker et al.*, 1980; *Baker*, 1992]. Our data suggest that substorms are not the only mechanism for this sporadic energy release.

Acknowledgments. We thank John Samson for helpful discussions and Bill Bristow for contributing to the Goose Bay data analysis. The EISCAT cross-magnetograms were supplied by R. Pellinen at the Finnish Meteorological Institute and the IMF data from R. Lepping at NASA. The Johns Hopkins University Applied Physics Laboratory HF radar at Goose Bay, Labrador, is supported in part by the National Science Foundation (NSF) division of Atmospheric Sciences under grant ATM-9003860, and in part by the National Aeronautics and Space Administration (NASA) under grant NAG5-1099. The Sondrestrom incoherent scatter radar is supported through NSF cooperative agreement ATM 8822500. This work was also supported by NSF grants ATM 90-17637, 90-17725, and 91-02439; and by the Air Force Office of Scientific Research contract F49620-92-C-0011.

The Editor thanks D. Weimer and J. M. Bosqued for their assistance in evaluating this paper.

REFERENCES

Akasofu, S.-I., P. D. Perreault, F. Yasuhara, and C.-I. Meng, Auroral substorms and the interplanetary magnetic field, *J. Geophys. Res.*, *78*, 7490, 1973.

Ashour-Abdalla, M., L. M. Zelenyi, J. M. Bosqued, and R. A. Kovrazhkin, Precipitation of fast ion beams from the plasma sheet boundary layer, *Geophys. Res. Lett.*, *19*, 617, 1992.

Baker, D. N., Driven and unloading aspects of magnetospheric substorms, Proceedings of the First International Conference on Substorms, Kiruna, Sweden, 23-27 March 1992, *Eur. Space Agency Spec. Publ.*, *SP-355*, 1992.

Baker, D. N., T. A. Fritz, R. L. McPherron, D. H. Fairfield, Y. Kamide, and W. Baumjohann, Magnetotail energy storage and release during the CDAW 6 substorm analysis intervals, *J. Geophys Res.*, *90*, 1205, 1985.

Baker, D. N., A. J. Klimas, R. L. McPherron, and J. Büchner, The evolution from weak to strong geomagnetic activity: An interpretation in terms of deterministic chaos, *Geophys. Res. Lett.*, *17*, 41, 1990.

Baker, D. N., A. J. Klimas, and D. A. Roberts, Examination of time-variable input effects in a nonlinear analogue magnetosphere model, *Geophys. Res. Lett.*, *18*, 1631, 1991.

Baker, K. B., and S. Wing, A new magnetic coordinate system for conjugate studies of high latitudes, *J. Geophys. Res.*, *94*, 9139, 1989.

Bargatze, L. F., D. N. Baker, R. L. McPherron, and E. W. Hones, Jr., Magnetospheric impulse response for many levels of geomagnetic activity, *J. Geophys. Res.*, *90*, 6387, 1985.

Bosqued, J. M., AUREOL-3 results on ion precipitation, *Phys. Scr.*, *18*, 158, 1987.

de la Beaujardière, O., and R. A. Heelis, Velocity spike at the poleward edge of the auroral zone, *J. Geophys. Res.*, *89*, 1627, 1984.

de la Beaujardière, O., R. Vondrak, and M. Baron, Radar observations of electric fields and currents associated with auroral arcs, *J. Geophys. Res.*, *82*, 5051, 1977.

de la Beaujardière, O., L. R. Lyons, and E. Friis-Christensen, Sondrestrom radar measurements of the reconnection electric field, *J. Geophys. Res.*, *96*, 13,907, 1991.

Eastman, T. E., B. Popielawska, and L. A. Frank, Three-dimensional plasma observations near the outer magnetospheric boundary, *J. Geophys. Res.*, *90*, 9519, 1985.

Fasel, G. J., J. I. Minow, R. W. Smith, C. S. Deehr, and L. C. Lee, Multiple brightenings of transient dayside auroral forms during oval expansions, *Geophys. Res. Lett.*, *24*, 2429, 1992.

Foster, J. C., J. M. Holt, R. G. Musgrove, and D. S. Evans, Ionospheric convection associated with discrete levels of particle precipitation, *Geophys. Res. Lett.*, *13*, 656, 1986.

Galperin, Y. I., and Y. I. Feldstein, Auroral luminosity and its relationship to magnetospheric plasma domains, in *Auroral Physics*, edited by C.-I. Meng, M. J. Rycroft, and L. A. Frank, p. 207, Cambridge University Press, New York, 1991.

Greenwald, R. A., K. B. Baker, R. A. Hutchins, and C. Hanuise, An HF phased-array radar for studying small-scale structure in the high-latitude ionosphere, *Radio Sci.*, *20*, 63, 1985.

Hardy, D. A., L. K. Schmitt, M. S. Gussenhoven, F. J. Marshall, H. C. Yeh, T. L. Shumaker, A. Hube, and J. Pantazis, Precipitating electron and ion detectors (SSJ/4) for the block 5D/Flights 6-10 DMSP satellites: Calibration and data presentation, *Rep. AFGL-TR-84-0317*, Air Force Geophys. Lab., Hanscom Air Force Base, Mass., 1984.

Hoffman, R. A., M. Sugiura, N. C. Maynard, R. M. Candey, J. D. Craven, and L. A. Frank, Electrodynamic patterns in the polar region during periods of extreme magnetic quiescence, *J. Geophys. Res.*, *93*, 14,515, 1988.

Kelly, J. D., Sondrestrom radar—initial results, *Geophys. Res. Lett.*, *10*, 1112, 1983.

Kerns, K. J., and M. S. Gussenhoven, Solar wind conditions for a quiet magnetosphere, *J. Geophys. Res.*, *95*, 20,867, 1990.

Klimas, A. J., D. N. Baker, D. A. Roberts, D. H. Fairfield, and J. Büchner, A nonlinear dynamical analogue model of geomagnetic activity, *J. Geophys Res.*, *97*, 12,253, 1992.

Lockwood, M., P. E. Sandholt, and S. W. H. Cowley, Dayside auroral activity and magnetic flux transfer from the solar wind, *Geophys. Res. Lett.*, *16*, 33, 1989.

Luhmann, J. G., R. J. Walker, C. T. Russell, N. U. Crooker, J. R. Spreiter, and S. S. Stahara, Patterns of magnetic field merging sites on the magnetopause, *J. Geophys. Res.*, *89*, 1739, 1984.

Lundin, R., I. Sandahl, J. Woch, M. Yamauchi, R. Elphinstone, and J. S. Murphree, Boundary layer driven magnetospheric substorms, Proceedings of the First International Conference on Substorms, Kiruna, Sweden, 23-27 March 1992, *Eur. Space Agency Spec. Publ.*, *SP-335*, 1992.

Lyons, L. R., Formation of auroral arcs via magnetosphere-ionosphere coupling, *Rev. Geophys.*, *30*, 93, 1992.

Lyons, L. R., and T. W. Speiser, Evidence for current sheet acceleration in the geomagnetic tail, *J. Geophys. Res.*, *87*, 2276, 1982.

Newell, P. T., S. Wing, C.-I. Meng, and S. Sigillito, The auroral oval position, structure and intensity of precipitation from 1984 onward: an automated on-line data base, *J. Geophys. Res.*, *96*, 5877, 1990.

Pudovkin, M.I., Physics of magnetospheric substorms: a review, in *Magnetospheric Substorms, Geophys. Monogr. Ser.*, vol. 64, edited by J. R. Kan, T. A. Potemra, S. Kokubun, and T. Iijima, pp. 17-27, AGU, Washington, D.C., 1991.

Rostoker, G., S.-I. Akasofu, J. Foster, R. A. Greenwald, Y. Kamide, K. Kawasoke, A. T. Y. Lui, R. L. McPherron, and C. T. Russell,

Magnetospheric substorms—definition and signatures, *J. Geophys. Res.*, 85, 1663, 1980.

Ruohoniemi, J. M., R. A. Greenwald, K. B. Baker, J.-P. Villain, and M. A. McCready, Drift motions of small-scale irregularities in the high-latitude *F* region: An experimental comparison with plasma drift motions, *J. Geophys. Res.*, *92*, 4553, 1987.

Ruohoniemi, J. M., R. A. Greenwald, K. B. Baker, and J. C. Samson, HF radar observations of Pc 5 field line resonances in the midnight/early morning MLT sector, *J. Geophys. Res.*, *96*, 15,697, 1991.

Samson, J. C., L. R. Lyons, P. T. Newell, F. Creutzberg, and B. Xu, Proton aurora and substorm intensifications, *Geophys. Res. Lett.*, *21*, 267, 1992.

Sandahl, I., and P.-A. Lindqvist, Electron populations above the nightside auroral oval during magnetic quiet times, *Planet. Space Sci.*, *38*, 1031, 1990.

Sandholt, P. E., Dayside auroral activity and magnetospheric boundary layer phenomena, *J. Geomagn. Geoelectr.*, *42*, 711-726, 1990.

Sergeev, V. A., A. G. Yahnin, R. A. Rakhmatulin, S. I. Solovjev, F. S. Mozer, D. J. Williams, and C. T. Russell, Permanent flare activity in the magnetosphere during periods of low magnetic activity in the auroral zone, *Planet. Space Sci.*, *34*, 1169, 1986.

Sergeev, V. A., O. A. Aulamo, R. J. Pellinen, M. K. Vallinkoski, T. Bösinger, C. A. Cattell, R. C. Elphic, and D. J. Williams, Non-substorm transient injection events in the ionosphere and magnetosphere, *Planet. Space Sci.*, 38, 231, 1990.

Weimer, D. R., Characteristic time scales of substorm expansion and recovery, Proceedings of the International Conference on Substorms, Kiruna, Sweden, 23-27 March 1992, 581, *Eur. Space Agency Spec. Publ., SP-355*, 1992.

Williams, P. J. S., R. V. Lewis, T. S. Virdi, M. Lester, and E. Nielsen, Plasma flow bursts in the auroral electrojets, *Ann. Geophys.*, in press, 1993.

Winningham, J. D., C. D. Anger, G. G. Shepard, D. J. Weber, and R. A. Wagner, The latitudinal morphology of 10-eV to 10-deV electron fluxes during magnetically quiet and disturbed times in the 2100-0300 MLT sector, *J. Geophys. Res.*, *80*, 3148, 1975.

Zelenyi, L. M., R. A. Krovazkhin, and J. M. Bosqued, Velocity-dispersed ion beams in the nightside auroral zone: AUREOL 3 observations, *J. Geophys. Res.*, *95*, 12,119, 1990.

O. de la Beaujardière, SRI International, 333 Ravenswood Avenue, Menlo Park, CA 94025.

E. Friis-Christensen and C. Danielsen, Hollandervaenget II, Dragoer, 2791, Denmark.

L. R. Lyons, Environmental Technology Center, Aerospace Corporation, Los Angeles, CA 90009.

P. T. Newell and J. M. Ruohoniemi, Applied Physics Laboratory, Johns Hopkins University, Laurel, MD 20723.

F. J. Rich, Geophysics Directorate, Phillips Laboratory, Hanscom Air Force Base, MA 01731.

(Received February 16, 1993;
revised May 25, 1993;
accepted July 9, 1993.)